# Oms1 associates with cytochrome *c* oxidase assembly intermediates to stabilize newly synthesized Cox1

Bettina Bareth[a], Miroslav Nikolov[b,†], Isotta Lorenzi[a], Markus Hildenbeutel[c,‡], David U. Mick[a], Christin Helbig[a], Henning Urlaub[b,d], Martin Ott[c], Peter Rehling[a,e,*], and Sven Dennerlein[a]

[a]Department of Cellular Biochemistry, University Medical Center Göttingen, D-37073 Göttingen, Germany; [b]Bioanalytical Mass Spectrometry Group, Max Planck Institute for Biophysical Chemistry and [e]Max Planck Institute for Biophysical Chemistry, D-37077 Göttingen, Germany; [c]Center for Biomembrane Research, Department of Biochemistry and Biophysics, Stockholm University, 106 91 Stockholm, Sweden; [d]Bioanalytik Group, Department of Clinical Chemistry, University Medical Center Göttingen, D-37075 Göttingen, Germany

**ABSTRACT** **The mitochondrial cytochrome *c* oxidase assembles in the inner membrane from subunits of dual genetic origin. The assembly process of the enzyme is initiated by membrane insertion of the mitochondria-encoded Cox1 subunit. During complex maturation, transient assembly intermediates, consisting of structural subunits and specialized chaperone-like assembly factors, are formed. In addition, cofactors such as heme and copper have to be inserted into the nascent complex. To regulate the assembly process, the availability of Cox1 is under control of a regulatory feedback cycle in which translation of *COX1* mRNA is stalled when assembly intermediates of Cox1 accumulate through inactivation of the translational activator Mss51. Here we isolate a cytochrome *c* oxidase assembly intermediate in preparatory scale from *coa1*Δ mutant cells, using Mss51 as bait. We demonstrate that at this stage of assembly, the complex has not yet incorporated the heme *a* cofactors. Using quantitative mass spectrometry, we define the protein composition of the assembly intermediate and unexpectedly identify the putative methyltransferase Oms1 as a constituent. Our analyses show that Oms1 participates in cytochrome *c* oxidase assembly by stabilizing newly synthesized Cox1.**

**Monitoring Editor**
Thomas D. Fox
Cornell University

Received: Dec 1, 2015
Revised: Mar 23, 2016
Accepted: Mar 24, 2016

## INTRODUCTION

The eukaryotic cytochrome *c* oxidase is a copper–heme *a* oxidase that acts as the terminal enzyme of the respiratory chain. The enzyme complex is composed of subunits of dual genetic origin. In yeast and humans, Cox1, Cox2, and Cox3 are multispanning inner membrane proteins encoded by the mitochondrial genome that form the core of the complex. These proteins are translated on membrane-associated ribosomes on the matrix side of the inner membrane and have to be inserted into the lipid phase by the mitochondrial protein export machinery. Oxa1 represents the core subunit of this mitochondrial export machinery. The channel-forming Oxa1 protein facilitates the membrane insertion of mitochondria-encoded proteins in a cotranslational manner (Jia *et al.*, 2003; Szyrach *et al.*, 2003; Krüger *et al.*, 2012). During this process, Oxa1 cooperates with the ribosome associate peripheral membrane protein Mba1 (Ott *et al.*, 2006; Pfeffer *et al.*, 2015). Mba1 is positioned close to the ribosomal exit tunnel and has been suggested to help to align the ribosome with the export machinery (Ott *et al.*, 2006; Bauerschmitt *et al.*, 2010; Pfeffer *et al.*, 2015). A multicopy suppressor screen revealed Oxa1 multicopy suppressor (Oms1; YDR316w) as an Oxa1-related protein that suppresses Oxa1 mutant alleles

This article was published online ahead of print in MBoC in Press (http://www.molbiolcell.org/cgi/doi/10.1091/mbc.E15-12-0811) on March 30, 2016.

The authors declare no competing financial interests.

Present addresses: †Gene Center, Ludwig-Maximilians-Universität, D-81377 Munich, Germany; ‡Institute for Cell and Gene Therapy and Centre for Chronic Immunodeficiency, Medical Centre, University of Freiburg, D-79106 Freiburg, Germany.

*Address correspondence to: Peter Rehling (Peter.Rehling@medizin.uni-goettingen.de)

Abbreviations used: BN–PAGE, blue native PAGE; HPLC, high-performance liquid chromatography; MS, mass spectrometry; SILAC, stable isotopes labeling by amino acids in cell culture.





Supplemental Material can be found at:
http://www.molbiolcell.org/content/suppl/2016/03/28/mbc.E15-12-0811v1.DC1.html

when overexpressed. Of interest, Oms1 contains a predicted C-terminal methyltransferase domain, mutations of which abolish its suppression capabilities (Lemaire *et al.*, 2004). However, the function of Oms1 has remained enigmatic.

The assembly of the cytochrome *c* oxidase represents a process during which the individual subunits associate in a sequential manner. The assembly process initiates on the membrane-inserted Cox1 protein, which associates transiently with diverse assembly factors and structural subunits to eventually form the active enzyme complex. Several factors in yeast and human mitochondria assist at different steps of the assembly process. Some of these have been functionally linked to distinct assembly intermediates and maturation processes. The identification and characterization of these assembly factors have significantly contributed to our understanding of the assembly process and provided insight into the molecular basis of assembly defects that lead to human disorders caused by cytochrome *c* oxidase deficiency (Fernández-Vizarra *et al.*, 2009; Mick *et al.*, 2011; Soto *et al.*, 2012; Herrmann *et al.*, 2013).

The assembly of the cytochrome *c* oxidase has been best analyzed in the yeast *Saccharomyces cerevisiae*. In yeast, translation of the *COX1* mRNA requires the dedicated translational activators Pet309, Pet54, Mam33, and Mss51 (Decoster *et al.*, 1990; Manthey and McEwen, 1995; Barrientos *et al.*, 2002; Pérez-Martínez *et al.*, 2003; Roloff and Henry, 2015; Mayorga *et al.*, 2016). After membrane insertion, the newly synthesized Cox1 associates with the assembly factors Coa3 and Cox14, which stabilize Cox1 (Glerum *et al.*, 1995; Barrientos *et al.*, 2004; Mick *et al.*, 2010; Fontanesi *et al.*, 2011). The Coa3/Cox14/Cox1 complex subsequently engages with the assembly factors Coa1 and Shy1 (Mick *et al.*, 2007; Pierrel *et al.*, 2007). Recruitment of Mss51 to Cox1 assembly intermediates inactivates Mss51, rendering it incompetent to support translation of Cox1. On further maturation of the assembly intermediate, Mss51 dissociates from the nascent cytochrome *c* oxidase and can stimulate further rounds of *COX1* mRNA translation (Barrientos *et al.*, 2002, 2004; Pérez-Martínez *et al.*, 2003; Mick *et al.*, 2007; Pierrel *et al.*, 2007). Of interest, in this process, loss of the assembly factor Coa1 can be suppressed by an increase in the amount of Mss51 and copper supplementation to the growth medium (Pierrel *et al.*, 2007). The loss of cytochrome *c* oxidase in *coa1*Δ cells is not explained by reduced Cox1 translation (Mick *et al.*, 2007; Pierrel *et al.*, 2007) but instead by a block in the assembly process, since newly synthesized Cox1 accumulates in an undefined assembly intermediate that contains Mss51 (Khalimonchuk *et al.*, 2010; Mick *et al.*, 2010).

Here we purified and analyzed an Mss51-containing cytochrome *c* oxidase assembly intermediate that accumulates in *coa1*Δ mitochondria. We demonstrate that Oms1 associates with this early assembly intermediate. Our analyses of the function of Oms1 show that it participates in cytochrome *c* oxidase assembly but that this function is independent of its putative methyltransferase domain. Analysis of *oms1*Δ mitochondria revealed a role of Oms1 in early steps of cytochrome *c* oxidase assembly and in the stabilization of newly synthesized Cox1. On the basis of our findings and the proposed genetic interaction between Oms1 and Oxa1, we suggest that Oms1 is an early assembly factor of cytochrome *c* oxidase and is involved in the first phases of the Cox1 life cycle and that stabilizes it after translation.

## RESULTS

### Oms1 is a constituent of COA complexes

Cytochrome *c* oxidase assembly progresses through multiple transient assembly intermediates. Owing to their low abundance at steady state, the protein composition of individual assembly intermediates has remained ill defined despite the fact that many of their constituents are known. Previous studies indicated that a lack of the assembly factor Coa1 leads to accumulation of newly synthesized Cox1 in an assembly intermediate (termed $COA^{220}$ in this study; Khalimonchuk *et al.*, 2010; Mick *et al.*, 2010). This $COA^{220}$ complex was reminiscent of a previously described Mss51-containing complex (Bareth *et al.*, 2013). On the basis of these observations, we expressed a C-terminally streptavidin- and FLAG-tagged Mss51 ($Mss51^{SF}$) in wild-type and *coa1*Δ backgrounds to purify the $COA^{220}$ complex. Functionality of this fusion construct was assessed by growth tests of $Mss51^{SF}$-expressing cells on fermentable (yeast extract/peptone/glucose [YPD]) and nonfermentable (yeast extract/peptone/glycerol [YPG]) carbon sources. Wild-type cells expressing $Mss51^{SF}$ from the chromosomal locus displayed wild type–like growth behavior on both carbon sources (Figure 1A). As expected, *coa1*Δ cells expressing $Mss51^{SF}$ failed to grow on nonfermentable medium (Mick *et al.*, 2007; Pierrel *et al.*, 2007). In addition, $Mss51^{SF}$-expressing wild-type cells displayed similar mitochondrial protein levels to wild-type mitochondria containing untagged Mss51 (Figure 1B). Thus we concluded that $Mss51^{SF}$ was functional and could be used for further analyses.

To establish an unbiased identification strategy allowing for a comprehensive identification of proteins present in the $COA^{220}$ complex, we generated an *arg4*Δ*coa1*Δ$Mss51^{SF}$ strain and performed stable isotope labeling by amino acids in cell culture (SILAC; Ong *et al.*, 2002). To avoid false-positive identifications, we carried out label-switch experiments in which $Mss51^{SF}$ isolations were performed after switching the medium from heavy to light amino acids between *arg4*Δ*coa1*Δ$Mss51^{SF}$ and the control strain (Figure 1C). Mass spectrometric analysis revealed selective enrichment of early cytochrome *c* oxidase–associated factors (Figure 1D and Supplemental Table S1). Of note, the cytochrome *c* oxidase core subunit Cox1 was the most enriched protein. Furthermore, the previously described cytochrome *c* oxidase assembly factor Shy1, the structural subunits Cox6 and Cox5, and the mitochondrial chaperone Ssc1 were identified. Peptides of Coa3 and Cox14 were not detected during liquid chromatography–tandem mass spectrometry analysis, probably due to their low molecular weight and hydrophobicity. Most interestingly, Oms1, a protein containing a predicted methyltransferase domain, was significantly enriched with $Mss51^{SF}$.

In conclusion, these analyses defined Mss51-interacting proteins. In addition to the early cytochrome *c* assembly factors and structural subunits, the Oms1 protein was identified as an Mss51-associated protein.

### $COA^{220}$ represents a heme-free intermediate

To confirm the SILAC analysis, we solubilized mitochondria derived from wild-type and $Mss51^{SF}$ cells, purified $Mss51^{SF}$-containing complexes, and analyzed eluates by SDS–PAGE and Western blotting. $Mss51^{SF}$ was efficiently isolated, as were early cytochrome *c* oxidase assembly factors (e.g., Shy1), the core subunit Cox1, and early-assembling nuclear-encoded subunits (e.g., Cox5 and Cox6; Figure 2A). Although Coa3 and Cox14 were not enriched in the SILAC mass spectrometric analysis (Figure 1D), we clearly detected them by Western blotting (Figure 2A). To define the $Mss51^{SF}$-containing complex in *coa1*Δ mitochondria, we isolated $Mss51^{SF}$ under native conditions and analyzed the eluted protein complexes by blue native (BN)-PAGE. Mss51 was solely detected in a complex of 220 kDa (named $COA^{220}$) together with Cox1, Cox14, and Cox5 (Figure 2B).

Shy1 and its mammalian homologue, SURF1, have been implicated in heme insertion into Cox1 (Bundschuh *et al.*, 2009).

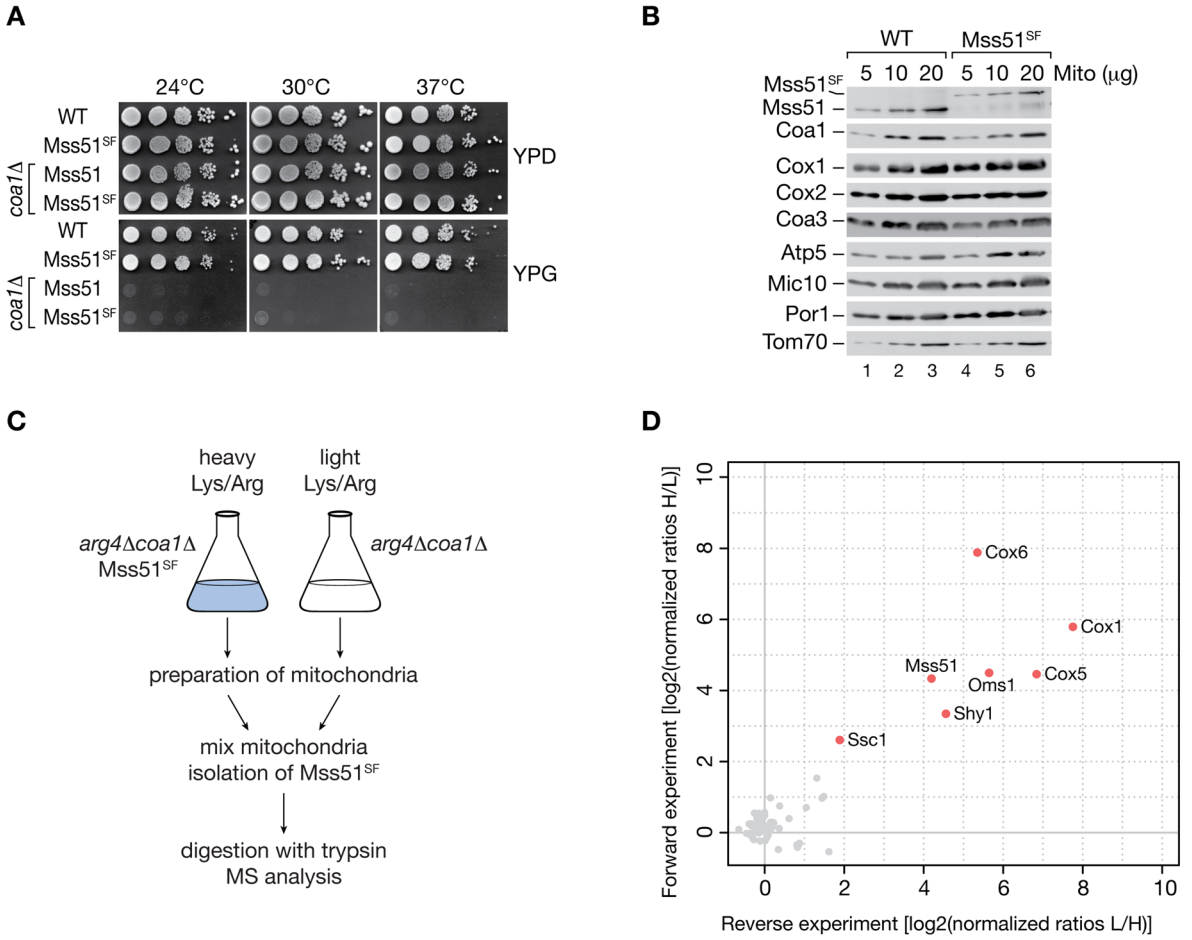


FIGURE 1: Oms1 interacts with Mss51. (A) Growth test on fermentable (YPD) and nonfermentable (YPG) full media. Cells were spotted in serial 10-fold dilutions and incubated at indicated temperatures. (B) Steady-state protein analysis from WT and Mss51-streptavidin-FLAG (Mss51$^{SF}$) mitochondria. Indicated amounts of isolated mitochondria (Mito) were separated by SDS–PAGE, followed by Western blotting, and probed for indicated mitochondrial proteins. (C) Schematic illustration of Mss51$^{SF}$ isolation for SILAC and mass spectrometry analysis. Representation of the forward experiment. For the reverse experiment, *arg4Δ/coa1Δ*/Mss51$^{SF}$ was grown on light medium and *arg4Δcoa1Δ* on heavy medium. (D) Scatterplot representation of normalized heavy/light (forward experiment) and light/heavy (reverse experiment) SILAC ratios after isolation of Mss51$^{SF}$ (via StrepTactin Sepharose) from *arg4Δcoa1Δ*. Enriched proteins are displayed as red dots and other proteins in gray. The full list of identified proteins is given in Supplemental Table S1.

Hence the presence of Shy1 in the Cox1-containing COA$^{220}$ complex prompted us to assess the heme content of the purified COA$^{220}$ complex. To this end, we solubilized Mss51$^{SF}$-containing mitochondria with digitonin and isolated complexes under native conditions. For comparison, we purified respiratory chain supercomplexes. Heme was extracted as described in *Materials and Methods* and samples analyzed by high-performance liquid chromatography (HPLC). As expected, heme *a* and heme *b* were identified in respiratory chain supercomplexes (Figure 2C). However, in Mss51$^{SF}$-containing complexes isolated from *coa1Δ* mitochondria, we detected neither heme *a* nor heme *b*. To compensate for the reduced levels of Cox1 present in intermediates from *coa1Δ* compared with respiratory chain supercomplexes from wild-type cells, we used 20 times more material for complex isolations from these mutant mitochondria. On the basis of these analyses, we conclude that the COA$^{220}$ complex contains Cox1 and cytochrome *c* oxidase assembly factors; however, the heme cofactors have apparently not been inserted into the maturing enzyme at this stage.

## Respiratory chain supercomplexes are altered in *oms1Δ* mitochondria

The presence of Oms1 in the Mss51$^{SF}$-isolated COA$^{220}$ complex, as assessed by mass spectrometry, was unexpected. Oms1 has been described as a mitochondrial protein able to act as an Oxa1 suppressor (Lemaire *et al.*, 2004). To confirm that Oms1 and Mss51 were present in the same complex, we purified Mss51$^{SF}$ from digitonin-solubilized mitochondria. The expected cytochrome *c* oxidase assembly factors Coa1 and Coa3 coisolated with Mss51. In addition, Oms1 was recovered in the eluate (Figure 3A). To substantiate this finding, we performed the reverse experiment using an antibody directed against the C-terminus of Oms1 for complex isolation. After immunoprecipitation, Mss51 was clearly recovered in the eluate; however, Coa1 could not be detected in the precipitates (Figure 3B). Because Coa1 was identified with Mss51$^{SF}$ but not during immunoprecipitation using an antibody directed against the C-terminus of Oms1, we performed the reverse experiment with an antibody against Coa1. Besides Cox14, Coa3, and Cox1, Oms1 was also detected, suggesting the presence of Mss51, Coa1, and Oms1 in a complex (Figure 3C).

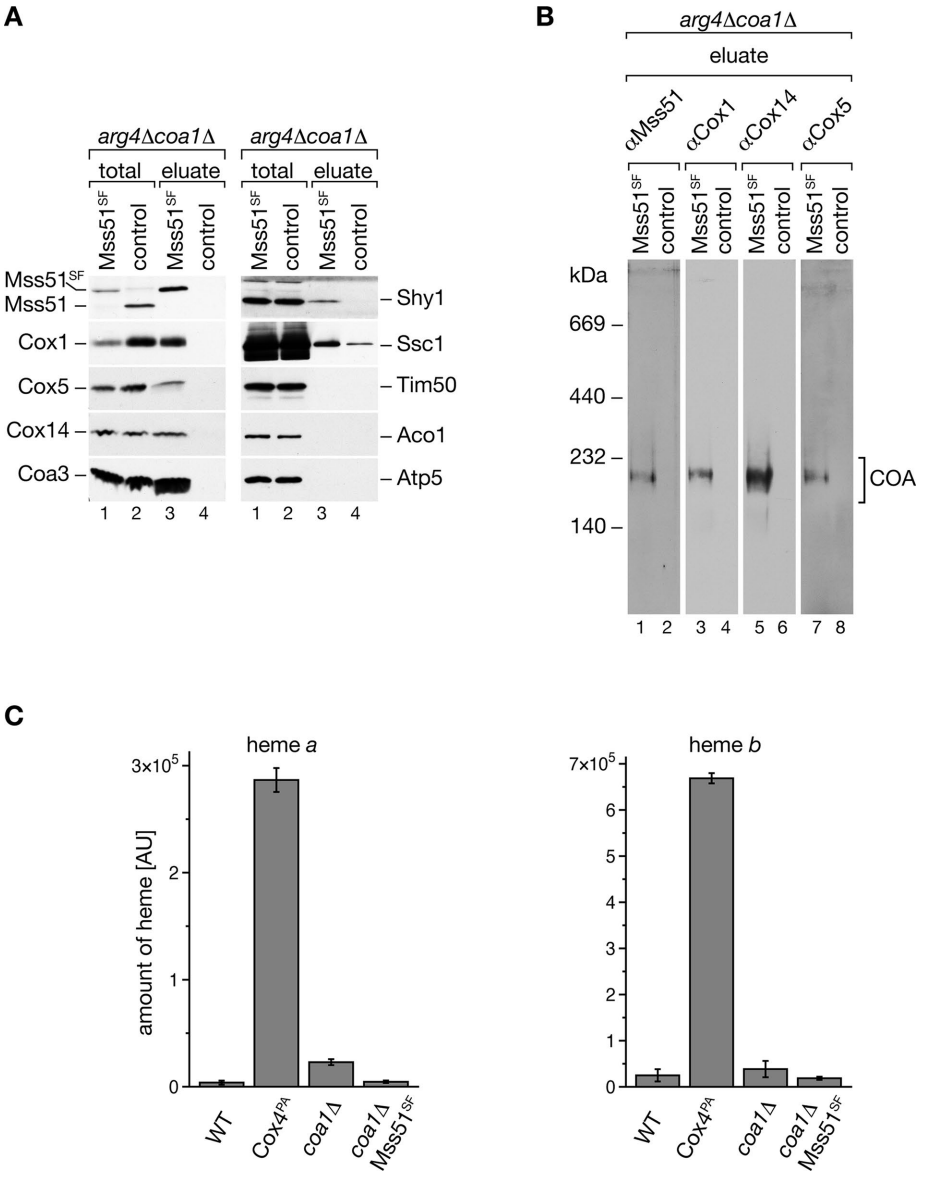


FIGURE 2: Characterization of the COA$^{220}$ complex in cells lacking Coa1. (A) Results of the SILAC analysis were confirmed by native purification of Mss51$^{SF}$-containing complexes. Eluates were separated by SDS–PAGE, followed by Western blot analysis. Amount of total sample loaded corresponds to 3% of the eluate. (B) Native eluted proteins (as in A) from *coa1Δ*/*arg4Δ*/Mss51$^{SF}$ mitochondria were analyzed by BN–PAGE and Western blotting. As a control, the purification was performed from solubilized *coa1Δarg4Δ* mitochondria. (C) HPLC analysis of heme *a* and heme *b* in isolated mature cytochrome *c* oxidase and COA complexes. Heme *a* and heme *b* were extracted and quantified from eluates of native isolated Cox4$^{ProtA}$ or Mss51$^{SF}$ complexes ($n = 3$, ±SEM).

To investigate the function of Oms1, we generated a strain with a chromosomal deletion of *OMS1* (*oms1Δ*) and assessed its growth behavior in comparison to wild-type and *coa1Δ* cells on full or synthetic media supplemented with fermentable (YPD/synthetic defined medium with glucose [SD]) or nonfermentable (YPG/synthetic defined medium with glycerol [SG]) carbon sources. After incubation at 24, 30, and 37°C, we observed the expected absence of growth of *coa1Δ* cells (Mick *et al.*, 2007; Pierrel *et al.*, 2007) and a subtle growth defect for *oms1Δ* cells on nonfermentable full medium (YPG) at 24 and 37°C compared with wild-type cells. The reduction in growth of *oms1Δ* cells was even more pronounced on synthetic media (Figure 3E). These findings suggested a respiratory chain defect in *oms1Δ* cells. Hence we analyzed *oms1Δ* mitochondria with regard to respiratory chain function. The analysis of steady-state protein levels revealed a clear reduction of Cox1 levels, whereas other tested proteins, such as Cox2, Coa1, and Coa3, were only mildly affected (Figure 3F).

To analyze respiratory chain complexes directly, we solubilized mitochondria and separated protein complexes by BN–PAGE. We observed a reduction of the $III_2$/$IV_2$ supercomplexes in *oms1Δ* mitochondria by Western blotting. At the same time, complex $III_2$ was apparent in mutant mitochondria samples (Figure 3G). No differences for complex V and $V_2$ were observed in these analyses (Figure 3G). To address whether the activity of respiratory chain complexes was affected, we conducted in-gel activity staining. In agreement with the observed rearrangement of supercomplexes, cytochrome *c* oxidase activity of the $III_2$/IV complex was increased compared with the wild-type sample, whereas reduced activity of the slower-migrating oligomer $III_2$/$IV_2$ was apparent in *oms1Δ* (Figure 3H). As a control, complex V activity remained unaltered in the mutant sample, confirming the immunoblotting results. As expected from the BN–PAGE analysis (Figure 3G), there was no difference in activity measurements of the cytochrome *c* reductase in *oms1Δ* mitochondria compared with wild type (Figure 3I, top). Because the cytochrome *c* oxidase, as the terminal enzyme of the respiratory chain, reduces molecular oxygen, we performed high-resolution oxygen measurements to follow $O_2$ consumption of wild-type and *oms1Δ* mitochondria. Oxygen consumption was significantly reduced in *oms1Δ* mitochondria (Figure 3I, bottom), indicating a respiratory defect. The results taken together show that Oms1 is necessary for proper function of the cytochrome *c* oxidase and mitochondrial respiration.

Previous analyses revealed that assembly factors of Cox1 might stay associated with Cox1 until the stage of supercomplex assembly. To address whether Oms1 was present in mitochondrial respiratory chain supercomplexes, we isolated Cor1$^{TAP}$-containing complexes under native conditions and analyzed copurifying proteins by Western blotting. In addition to the expected complex III and IV subunits, we recovered assembly factors (e.g., Cox14) and supercomplex-associated factors (e.g., Rcf2; Chen *et al.*, 2012; Strogolova *et al.*, 2012; Vukotic *et al.*, 2012). However, Oms1 was not identified in detectable amounts (Figure 3D). Thus we hypothesized that Oms1 is present only in the COA$^{220}$ complex.

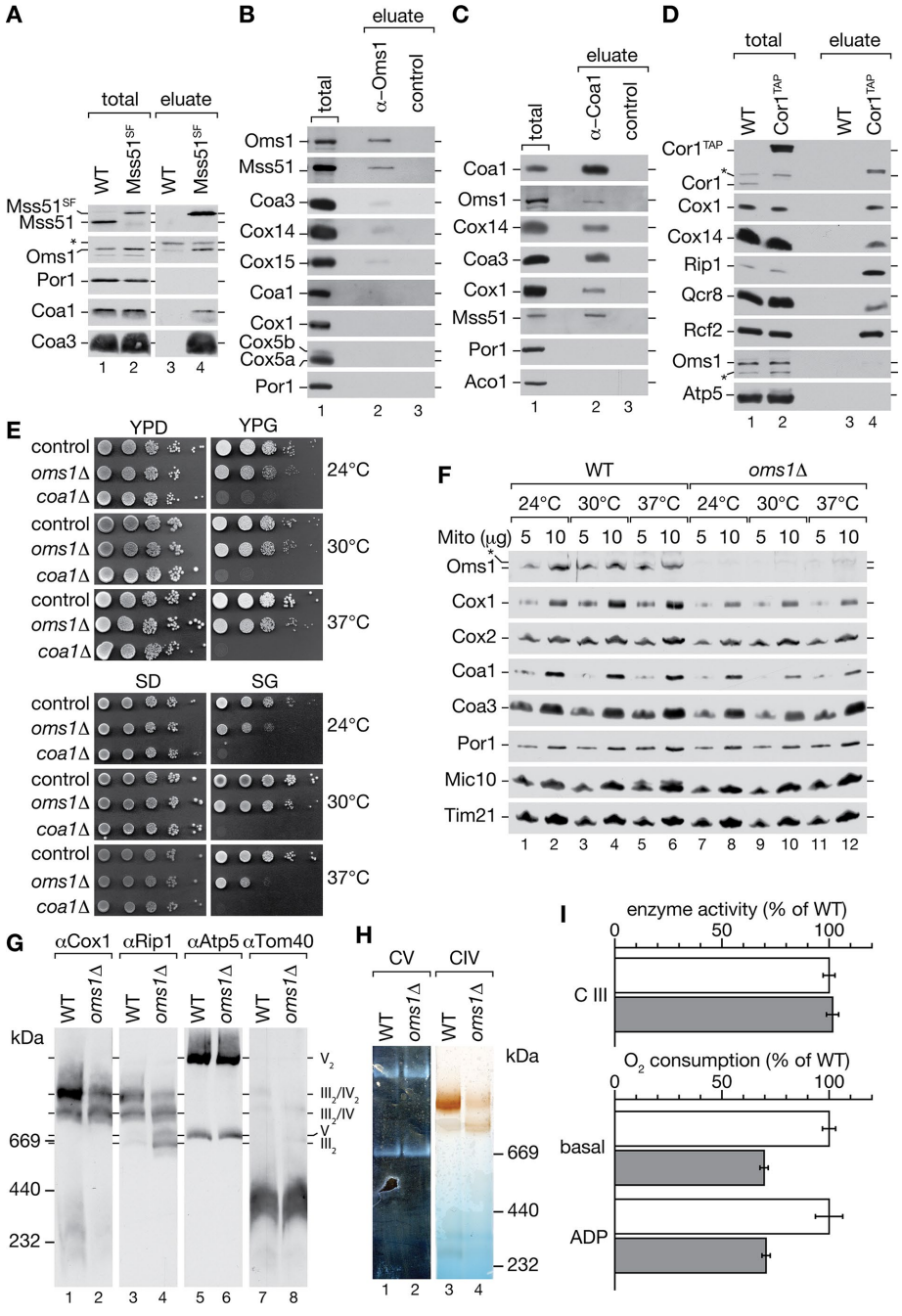


FIGURE 3: Loss of Oms1 effects mitochondrial supercomplexes. (A) WT and Mss51$^{SF}$ mitochondria were solubilized in 1% digitonin buffer and complexes purified by StrepTactin Sepharose chromatography. After acidic elution, the eluate was analyzed by SDS–PAGE and Western blotting (total 1.5%, eluate 100%). Asterisks indicates unspecific antibody signal. Coimmunoprecipitation of Oms1 (B) or Coa1 (C) and control from digitonin-solubilized mitochondria. Eluates were analyzed by SDS–PAGE and Western blotting (total 1.5%, eluate 100%). (D) Mitochondria were solubilized with digitonin-containing buffer and supercomplexes isolated via TAP-tagged Cor1 using IgG chromatography followed by TEV protease cleavage. Eluates were analyzed as in B (total, 10%; eluate, 100%). Asterisks indicate cross-reaction of the antibodies. (E) Growth test on fermentable and nonfermentable full (YPD, YPG) and synthetic (SD –Trp, SG –Trp) media. WT, *oms1*Δ, and *coa1*Δ cells were spotted in serial 10-fold dilutions and incubated at indicated temperatures. (F) Steady-state protein level analysis of WT and *oms1*Δ mitochondria isolated from cells grown in YPG at different temperatures (24, 30, 37°C). Indicated amounts of mitochondria (Mito) were separated by SDS–PAGE, followed by Western blotting. Western blot analysis (G) and in-gel activity staining for cytochrome *c* oxidase and $F_1F_o$ ATP-synthase (H) after BN–PAGE separation. Cells for mitochondrial preparation were grown on YPG at 30°C. (I) Top, enzymatic activity assay of cytochrome *c* reductase (CIII) in WT (white bars) and *oms1*Δ (gray bars) mitochondria ($n = 3$, ±SEM). Bottom, oxygen consumption measurement of mitochondria from WT (white bars) and *oms1*Δ (gray bars). Isolated mitochondria were incubated with NADH (basal) and successively combined with ADP (phosphorylating respiration; state 3) in a high-resolution respirometry chamber ($n = 4$, ±SEM).

## Mutations in the methyltransferase domain of Oms1 do not affect cytochrome *c* oxidase function

Oms1 contains a predicted methyltransferase domain that is critical for its functions as an Oxa1 suppressor (Lemaire *et al.*, 2004). This finding prompted us to investigate the function of the putative methyltransferase domain with regard to the observed cytochrome *c* oxidase defect. We used site-directed mutagenesis to create plasmids carrying the endogenous promoter and the *OMS1* open reading frame with the previously described methyltransferase-domain mutations (Lemaire *et al.*, 2004) as either single or combined mutations. In addition, we investigated effects of Oms1 overexpression (wild-type and mutant forms). The *oms1*Δ cells were either transfected with centromeric (pRS416) or high-copy (pRS426) plasmids carrying the different constructs. Because the growth defect of *oms1*Δ cells was most pronounced on synthetic media, we investigated cell growth on SD and SG media at various temperatures. As a control, we used *cox15*Δ cells transformed with the empty pRS416 plasmid. Although we observed the described growth phenotype of *oms1*Δ, all tested mutations were able to restore cell growth (Figure 4A). Subsequently, we isolated mitochondria from *oms1*Δ cells containing the empty plasmid or the wild-type (WT) *OMS1*-containing plasmid or expressing the double mutant of *OMS1* (encoding Oms1$^{DT>AA}$). Because deletion of *OMS1* led to an altered respiratory chain complex organization, we solubilized *oms1*Δ mitochondria containing an empty plasmid or the plasmid-encoded Oms1 variants in digitonin buffer and subjected the extracts to BN–PAGE and Western blotting. Expression of Oms1$^{WT}$ restored supercomplex formation in mitochondria. Surprisingly, the Oms1$^{DT>AA}$ protein also restored supercomplex formation to WT levels (Figure 4B). In addition, we performed oxygen consumption measurements of mitochondria from *oms1*Δ cells and cells expressing Oms1$^{WT}$ and Oms1$^{DT>AA}$. Whereas oxygen consumption in *oms1*Δ mitochondria was reproducible decreased, Oms1$^{WT}$ and

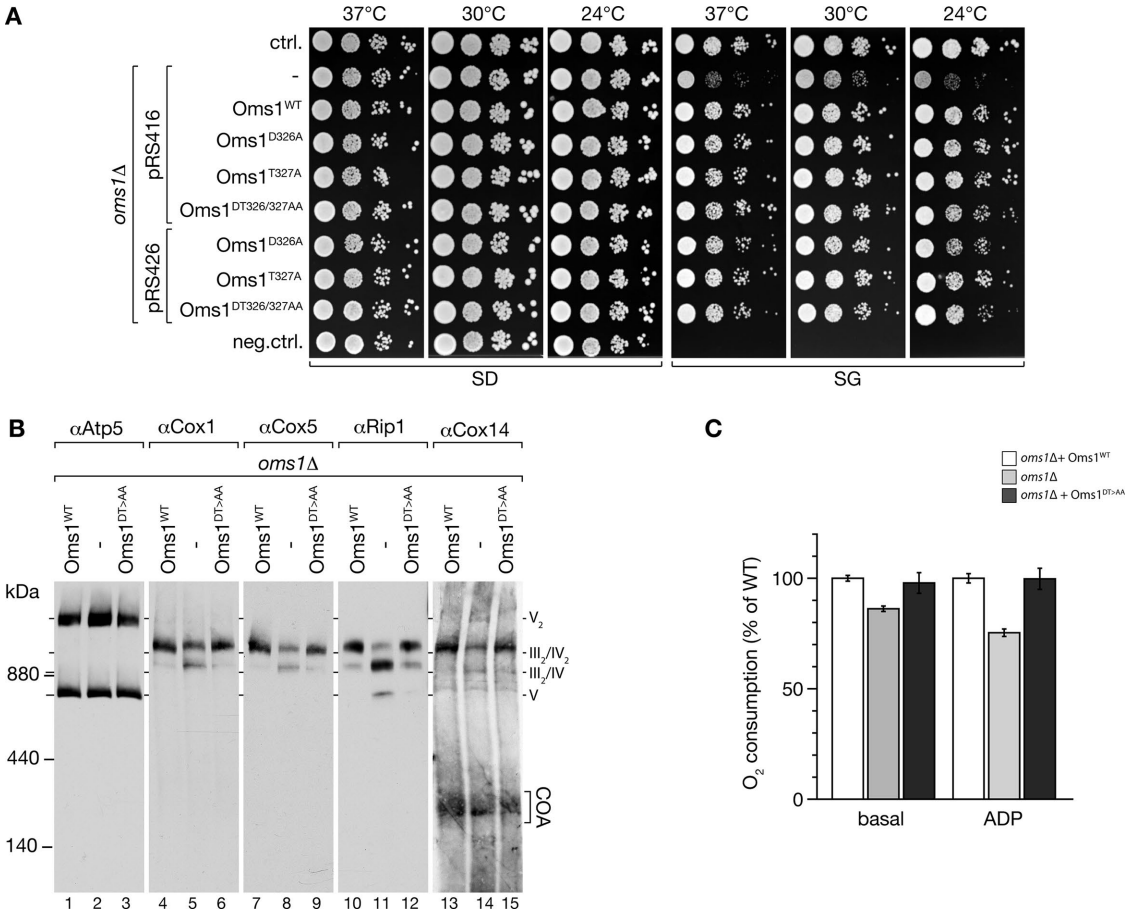


FIGURE 4: Analysis of the putative Oms1 methyltransferase domain. (A) Serial dilutions of *oms1*Δ cells containing an empty plasmid (–) or expressing WT Oms1 (Oms1$^{WT}$) or mutant variants of Oms1 (Oms1$^{D426A}$, Oms1$^{T427A}$, Oms1$^{DT426/427AA}$) were spotted on fermentable (SD) or nonfermentable (SG) solid synthetic medium and incubated at the indicated temperatures. All variants of Oms1 were cloned with the endogenous promoter and expressed either from a single copy (pRS416) for endogenous protein levels or from a multicopy plasmid (pRS426) for overexpression. As a control (ctrl.), WT cells carrying an empty pRS416 plasmid were used, and as a negative control (neg. ctrl.), *cox15*Δ cells carrying an empty pRS416 plasmid were used. (B) For analysis of mitochondrial OXPHOS complexes, mitochondria (Mito) isolated from cells containing an empty plasmid (–) or expressing either WT Oms1 or the double mutant variant of Oms1 (Oms1$^{DT426/427AA}$) were separated by BN–PAGE and analyzed by Western blotting. (*C*) Oxygen consumption of mitochondria quantified by high-resolution respirometry (at 30°C) in the presence of NADH (basal) or NADH and additional ADP (ADP). White bars, *oms1*Δ+ pRS416 (Oms1$^{WT}$); light gray bars, *oms1*Δ + pRS416; dark gray bars, *oms1*D+ pRS416 (Oms1$^{DT>AA}$). $n = 4$, ±SEM.

Oms1$^{DT>AA}$ mitochondria displayed similar oxygen consumption rates (Figure 4C). On the basis of these observations, we conclude that although mutations in the Oms1 methyltransferase domain are critical for suppression of Oxa1 mutants (Lemaire *et al.*, 2004), rearrangement of supercomplexes and reduced cytochrome *c* oxidase activity are functionally not linked to this domain.

### Oms1 stabilizes newly synthesized Cox1

We identified Oms1 as a protein copurifying with Mss51 under conditions of an accumulating early cytochrome *c* oxidase assembly intermediate. Loss of Oms1 leads to supercomplex rearrangements, reduced Cox1 steady-state levels, and reduced cytochrome *c* oxidase activity. Because assembly intermediates are short-lived under physiological conditions and of low abundance in mitochondria, we speculated that an interaction of Oms1 with COA$^{220}$ was likely transient in wild-type cells. To support this hypothesis, we carried out Oms1 immunoprecipitation analyses from mitochondrial extracts obtained from wild-type and *coa1*Δ mutant mitochondria with accumulated COA$^{220}$ complex. Oms1 was efficiently isolated from both extracts (Figure 5A). As expected, Mss51 and Coa3 were enriched in samples obtained from *coa1*Δ mitochondria, whereas a small amount of Mss51 was recovered in the wild-type sample at steady state (see also Figure 3B). Thus Mss51 coimmunoprecipitation efficiency correlated with the abundance of the COA$^{220}$ intermediate. To investigate further the interaction of Mss51 and Oms1 in early cytochrome *c* oxidase assembly steps, we performed Oms1 immunoprecipitations from *coa3*Δ, *cox14*Δ, and cox1$^{-}$ mitochondrial extracts. Mss51 could be detected only in the wild-type sample (Figure 5B). This observation suggests that Oms1 association with Mss51 depends on the presence of Cox1 and the formation of Cox1-containing assembly intermediates.

Because Mss51 is required for *COX1* mRNA translation and thus Cox1 expression, we analyzed whether lack of Oms1 affected Cox1 synthesis or stability. To investigate Cox1 synthesis in *oms1*Δ cells,

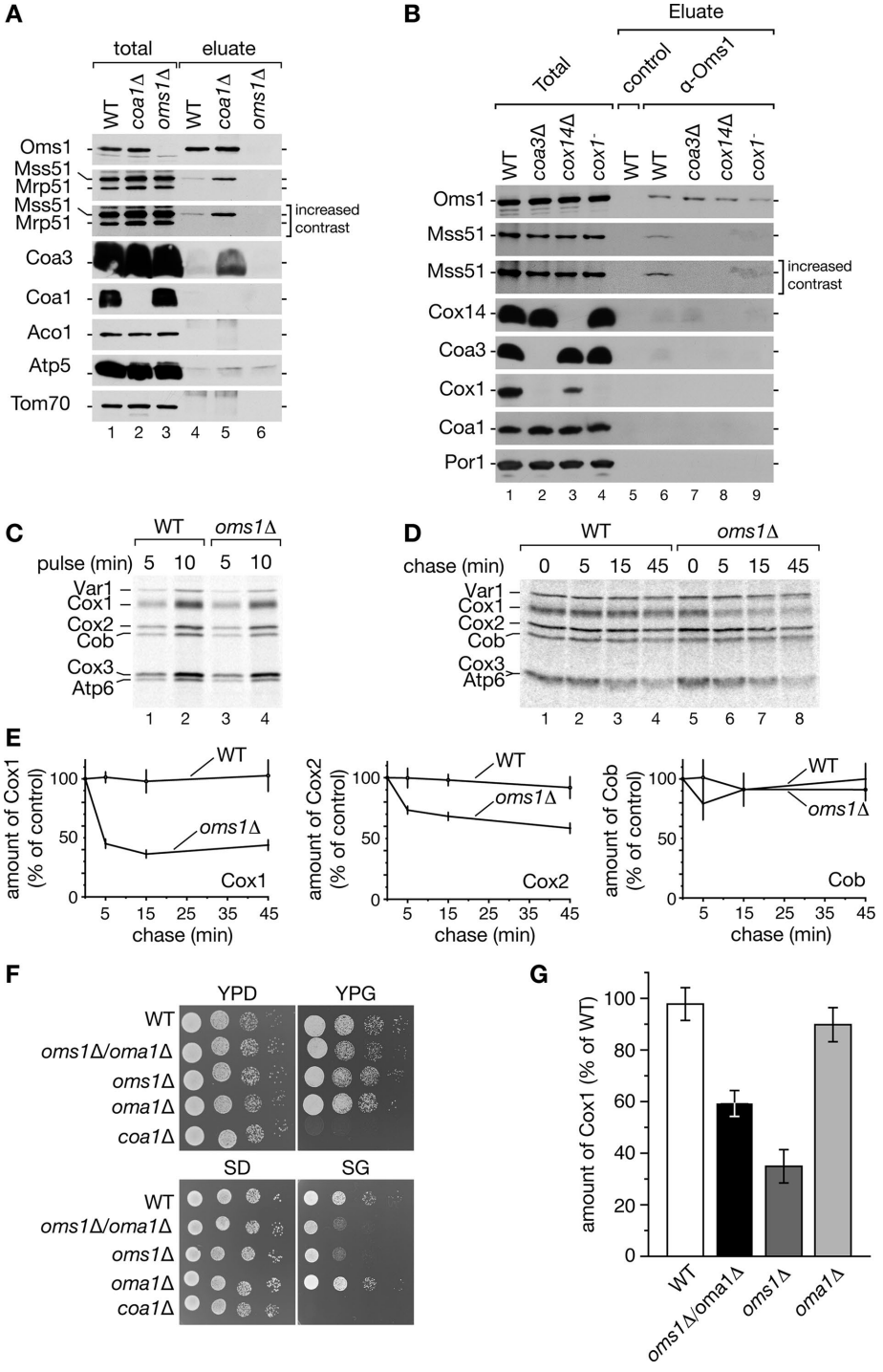


FIGURE 5: Oms1 acts in early steps of cytochrome *c* oxidase biogenesis. (A) Coimmunoprecipitation of Oms1 from digitonin-solubilized mitochondria isolated from WT, *coa1*Δ, and *oms1*Δ cells were analyzed by SDS–PAGE and Western blotting (total 1.5%, eluate 100%). (B) Immunoprecipitation of Oms1 as in A from WT, *coa3*Δ, *cox14*Δ, and *cox1*$^{-}$ mitochondria. Eluates were analyzed by SDS–PAGE and Western blotting (total 1%; eluate 100%). (C) In vivo pulse labeling of mitochondrial translation products using WT and *oms1*Δ cells. After [$^{35}$S] methionine labeling for 10 min at 30°C, whole-cell extracts were prepared and analyzed by SDS–PAGE and digital autoradiography. (D) Mitochondrial translation products were labeled with [$^{35}$S]methionine for 5 min as in C. Reactions were stopped by the addition of unlabeled methionine, and incubation continued at 30°C for the indicated chase times. Samples were processed as in C. (E) Signals of three independent experiments as shown in D were quantified using ImageQuant TL software. Bars represent the mean ratios of Cox1, Cox2, or Cob to Var1 relative to the signal after 0 min of chase (100%) for each individual strain ($n = 3$, ±SEM). (F) Growth test on fermentable and nonfermentable full (YPD, YPG) and synthetic (SD, SG) media. Yeast cells from the indicated strains were spotted in serial 10-fold dilutions and incubated at 30°C. (G) Quantification of in vivo labeling of mitochondrial translational products. Cells were labeled for 5 min and chased for 15 min. TCA-precipitated samples were separated by SDS–PAGE, quantified by digital autoradiography, and normalized for Var1 (C). $n = 3$; ± SEM.

we performed in vivo pulse labeling experiments. However, we did not observe any changes in mitochondrial protein synthesis in *oms1*Δ mitochondria (Figure 5C). Accordingly, the observed reduction in Cox1 that we observe in *oms1*Δ cells could not be attributed to defect in its synthesis. Alternatively, the reduced amount of Cox1 could be due to an increased turnover of Cox1. To address this, we pulse labeled mitochondrial translation products and analyzed labeled products after an extended chase. A significantly increased turnover rate of Cox1 was apparent in *oms1*Δ compared with wild-type cells and to a lesser extent also for Cox2 (Figure 5D). A quantitative analysis showed a degradation of Cox1 to 45% after a 5-min chase compared with the wild-type control but no further decrease during an extended chase of 45 min (Figure 5E). In addition, newly synthesized Cox2 displayed an increased turnover to 73% (after a 5-min chase) and to 58% (after 45 min). In contrast, Cob stability was not affected in *oms1*Δ cells. In conclusion, Oms1 is a transient interactor of Cox1 and present in the COA$^{220}$ complex. Although it is not required for Cox1 translation, Oms1 assists in stabilizing Cox1 during early steps of cytochrome *c* oxidase assembly. Because no protein involved in Cox2 maturation was found in the SILAC analysis together with Oms1 and Mss51 and previous reports also described destabilization of Cox2 when Cox1 is lacking (Barrientos *et al.*, 2002; Pérez-Martínez *et al.*, 2003; Mick *et al.*, 2007, 2010; Pierrel *et al.*, 2007, 2008; Fontanesi *et al.*, 2011), the decreased stability of Cox2 is probably indirect.

Lemaire *et al.* (2004) suggested that Oms1 might methylate Oxa1, rendering it resistant to Oma1 protease-mediated turnover, and hence support Cox1 biogenesis indirectly. Moreover, Bestwick *et al.* (2010) found in *coa2*Δ cells that instability of Cox1 could be overcome by deletion of *OMA1*. Hence, to test a role of Oma1 in the turnover of Cox1, we generated a chromosomal deletion of *OMA1* (*oma1*Δ) and a double-mutant strain lacking *OMS1* and *OMA1* (*oms1*Δ/*oma1*Δ). We assessed the growth

behavior of these strains on full or synthetic media containing fermentable (YPD/SD) or nonfermentable (YPG/SG) carbon sources. We used WT and *coa1*Δ cells as control. We reproducibly observed the growth defect of *oms1*Δ cells on nonfermentable media (Figure 5F). Whereas the single-mutant *oma1*Δ strain showed no growth defect, *oms1*Δ/*oma1*Δ cells displayed the same growth phenotype as *oms1*Δ cells (Figure 5F). To investigate Cox1 stability directly, we performed in vivo pulse labeling of mitochondrial translation products in *oma1*Δ and *oms1*Δ/*oma1*Δ cells in comparison to *oms1*Δ. Whereas Cox1 stability was significantly reduced in *oms1*Δ cells, we observed a subtle increase of Cox1 stability in the double *oms1*Δ/*oma1*Δ strain (Figure 5G). These analyses indicate that Oma1 contributes to the turnover of Cox1 in *oms1*Δ mutant mitochondria. However, in addition to Oma1, other proteases appear to be involved in this process.

## DISCUSSION

Assembly of the cytochrome *c* oxidase initiates with the synthesis of Cox1. After cotranslational insertion of the newly synthesized Cox1 into the inner mitochondrial membrane, the protein becomes stabilized through interactions with assembly factors such as Cox14 and Coa3 (Barrientos *et al.*, 2004; Pérez-Martínez *et al.*, 2009; Mick *et al.*, 2010; Fontanesi *et al.*, 2011). Current concepts on the assembly process suggest that in successive steps additional assembly factors associate, cofactors are inserted into Cox1, and nuclear- and mitochondria-encoded subunits are recruited (Taanman and Williams, 2001; Herrmann and Funes, 2005; Mick *et al.*, 2011; Fox, 2012; Soto *et al.*, 2012; Richter-Dennerlein *et al.*, 2015). Because assembly factors accompany Cox1 during successive stages of the assembly process, individual assembly intermediates are difficult to purify and therefore have not been defined biochemically. Here we used a *coa1*Δ mutant in which newly synthesized Cox1 forms a stable intermediate to isolate and dissect this complex (Khalimonchuk *et al.*, 2010; Mick *et al.*, 2010). Our analyses indicate that the purified $COA^{220}$ complex has not yet received the heme cofactors. In addition, we identified Oms1 as an unexpected constituent of the complex. Our analyses indicate that Oms1 is a transient interactor of the assembly pipeline, since we find only a significant interaction with assembly intermediates under conditions of an accumulating intermediate. It is interesting that Oms1 was linked previously to respiratory chain biogenesis, as it was identified as a suppressor of *OXA1* mutant alleles. In that case, the methyltransferase domain of Oms1 was shown to be critical for the suppression phenotype (Lemaire *et al.*, 2004). However, with regard to the *oms1*Δ growth defect that we observed and the underlying cytochrome *c* oxidase defect, we show that a functional methyltransferase domain is dispensable. These findings suggest that two distinct activities can be attributed to Oms1.

Although the molecular basis for the observed genetic interaction with Oxa1 remains unexplained, a lack of Oms1 affects the stability of newly synthesized Cox1. However, despite this defect, a significant amount of Cox1 is apparently maintained in an assembly-competent state. The reduction of Cox1 seen at steady state in *oms1*Δ mitochondria is much less pronounced than what is seen in *cox14*Δ or *coa3*Δ. Hence lack of Cox14 and Coa3 destabilizes Cox1, but at the same time, both proteins interact with the translational activator Mss51 and Cox1 early during the assembly process (Barrientos *et al.*, 2004; Pérez-Martínez *et al.*, 2009; Mick *et al.*, 2010; Fontanesi *et al.*, 2011). Our analyses indicate that although the association of Oms1 with $COA^{220}$ appears to be transient and much less apparent at steady state, an association of Oms1 with Mss51 can be detected when Coa1 is lacking. This finding suggests that Oms1 is primarily engaged with Mss51 and likely recruited to the $COA^{220}$ complex by Mss51. However, given the role of Mss51 in translation of Cox1, this hypothesis cannot easily be assessed experimentally. Moreover, it will be important to address whether Oms1 acts directly on Cox1 or affects stability indirectly via Cox14, Coa3, or another constituent of the $COA^{220}$ intermediate.

## MATERIALS AND METHODS

### Yeast strains, molecular cloning, and mitochondrial preparation

All *S. cerevisiae* strains, with the exception of *cox1*$^{-}$, used in this study are derived from YPH499 (Sikorski and Hieter, 1989) and listed in Table 1. Chromosomal deletions of *COA1*, *ARG4*, *OMA1*, *COA3*, *COX14*, and *OMS1*, double-mutant strains, and tagged versions of Mss51 were generated by introduction of the *TRP1*, *NatNT2,* or *His3MX6* cassettes using PCR-based strategies (Knop *et al.*, 1999; Janke *et al.* 2004). The *cox1*$^{-}$ yeast cells were cultured as described previously (Mick *et al.*, 2010). Streptavidin-FLAG–tagged Mss51 ($Mss51^{SF}$) was generated using a modified pYM2.1 vector (Alkhaja *et al.*, 2012). *OMS1* was cloned with its endogenous promoter and terminator from yeast (YPH499) genomic DNA into pRS416 and pRS426 (Stratagene). Point mutations were introduced by site-directed mutagenesis (QuikChange; Stratagene, Cambridge, United Kingdom) according to the manufacturer's specifications. Yeast strains were transformed using the lithium acetate method and confirmed by PCR or Western blot analysis. Yeast cells were grown in liquid medium containing 1% yeast extract, 2% peptone and 2% glucose, 1% galactose, or 3% glycerol (YPD/YPGal/YPG, respectively). Strains containing plasmid-borne wild-type or mutant form of *OMS1* were grown on synthetic medium (0.67% yeast nitrogen base, 0.07% complete supplement mixture –Ura) and 1% galactose. If not indicated otherwise, yeast cells were grown at 30°C. For growth tests, liquid precultures were adjusted to $OD_{600}$ 0.3, and serial 1:10 dilutions were spotted on solid media plates and incubated for 3–5 d at the indicated temperatures. Mitochondria were isolated essentially as previously described (Meisinger *et al.*, 2006). For steady-state analysis of mitochondrial proteins, different amounts of mitochondria were subjected to SDS–PAGE, followed by Western blot analysis.

### Native protein complex isolation

Mitochondria were solubilized in 20 mM Tris/HCl (pH 7.4), 100 mM NaCl, 10% (wt/vol) glycerol, 5 mM EDTA, 2 mM phenylmethylsulfonyl fluoride (PMSF), and 1% digitonin for 30 min at 4°C. The solubilized material was cleared (20,000 × *g*, 15 min, 4°C) and the mitochondrial extract applied to the respective resin for 1–2 h at 4°C. After extensive washing (20 mM Tris/HCl, pH 7.4, 100 mM NaCl, 10% [wt/vol] glycerol, 5 mM EDTA, 2 mM PMSF, 0.3% digitonin), bound material was eluted, mixed with the appropriate loading dye and analyzed by SDS- or BN–PAGE. For immunoglobulin G (IgG) chromatography of $Cox4^{ProtA}$ and $Cor1^{TAP}$, human IgGs (Sigma-Aldrich, St. Louis, MO) were coupled to CNBr-activated Sepharose (GE Healthcare, Little Chalfont, United Kingdom) according to the manufacturer's specifications. Bound material was eluted by tobacco etch virus (TEV) protease (Invitrogen, Carlsbad, CA) treatment. TEV protease carrying a polyhistidine tag was removed by addition of Ni–nitrilotriacetic acid (Rehling *et al.*, 2003).

Coimmunoprecipitation was performed as described (Hutu *et al.*, 2008; Mick *et al.*, 2010). Coa1- and Oms1-specific antisera were bound to Protein A–Sepharose (GE Healthcare) in 0.1 M potassium phosphate buffer (pH 7.4) for 1 h at room temperature and subsequently cross-linked with 5 mg/ml dimethyl pimelimidate (DMP) in 0.1 M sodium borate (pH 9.0) for 30 min at room temperature. DMP

| Strain | Genotype | Source |
|---|---|---|
| YPH499 | *Mat a, ade2-101 his3-Δ200 leu2-Δ1 ura3-52 trp1-Δ63 lys2-801* | Sikorski and Hieter, 1989 |
| *coa1Δ* (BBY06) | *Mat a, ade2-101 his3-Δ200 leu2-Δ1 ura3-52 trp1-Δ63 lys2-801*; *coa1*::*klTRP1* | This study |
| *coa3Δ* | *Mat a, ade2-101 his3-Δ200 leu2-Δ1 ura3-52 trp1-Δ63 lys2-801*; *coa3*::*HIS3MX6* | Mick *et al.*, 2010 |
| *cox14Δ* | *Mat a, ade2-101 his3-Δ200 leu2-Δ1 ura3-52 trp1-Δ63 lys2-801*; *cox14*::*HIS3MX6* | Mick *et al.*, 2010 |
| *shy1Δ* | *Mat a, ade2-101 his3-Δ200 leu2-Δ1 ura3-52 trp1-Δ63 lys2-801*; *shy1*::*HIS3MX6* | Mick *et al.*, 2007 |
| *oma1Δ* (931) | *Mat a, ade2-101 his3-Δ200 leu2-Δ1 ura3-52 trp1-Δ63 lys2-801*; *oma1*::*HIS3MX6* | This study |
| *cox1*$^{-}$ | *Mat α ade1 op1*; *cox1*-G421 | Mick *et al.*, 2007 |
| Mss51$^{strepFLAG}$ (BBY45) | *Mat a, ade2-101 his3-Δ200 leu2-Δ1 ura3-52 trp1-Δ63 lys2-801*; *mss51*::*mss51*-Strep-FLAG-*HIS3MX6* | This study |
| *coa1Δ* Mss51$^{StrepFLAG}$ (BBY09) | *Mat a, ade2-101 his3-Δ200 leu2-Δ1 ura3-52 trp1-Δ63 lys2-801*; *coa1*::*klTRP1*; *mss51*::*mss51*-Strep-FLAG-*HIS3MX6* | This study |
| *coa1Δ arg4Δ* (BBY12) | *Mat a, ade2-101 his3-Δ200 leu2-Δ1 ura3-52 trp1-Δ63 lys2-801*; *coa1*::*klTRP1*; *arg4*::*natNT2* | This study |
| *coa1Δ* Mss51$^{StrepFLAG}$ *arg4Δ* (BBY13) | *Mat a, ade2-101 his3-Δ200 leu2-Δ1 ura3-52 trp1-Δ63 lys2-801*; *coa1*::*klTRP1*; *mss51*::*mss51*-Strep-FLAG-*HIS3MX6*; *arg4*::*natNT2* | This study |
| Cor1$^{TAP}$ | *Mat a, his3-Δ1, leu2Δ0, met15Δ0, ura3Δ0*; *cor1*::*cor1*-TAP | Vukotic *et al.*, 2012 |
| Cox4$^{ProtA}$ | *Mat a, ade2-101 his3-Δ200 leu2-Δ1 ura3-52 trp1-Δ63 lys2-801*; *cox4*::*cox4*-TEV-ProtA-7HIS-*HIS3MX6* | Vukotic *et al.*, 2012 |
| *oms1Δ* (BBY28) | *Mat a, ade2-101 his3-Δ200 leu2-Δ1 ura3-52 trp1-Δ63 lys2-801*; *oms1*::*klTRP1* | This study |
| *oms1Δ oma1Δ* (932) | *Mat a, ade2-101 his3-Δ200 leu2-Δ1 ura3-52 trp1-Δ63 lys2-801*; *oms1*::*klTRP1*; *oma1*::*HIS3MX6* | This study |
| *oms1Δ* + pRS416 (BBY77) | *Mat a, ade2-101 his3-Δ200 leu2-Δ1 ura3-52 trp1-Δ63 lys2-801*; *oms1*::*klTRP1* [pRS416] | This study |
| *oms1Δ* + Oms1$^{WT}$ (BBY69) | *Mat a, ade2-101 his3-Δ200 leu2-Δ1 ura3-52 trp1-Δ63 lys2-801*; *oms1*::*klTRP1* [pRS416-OMS1] | This study |
| *oms1Δ* + Oms1$^{D326A}$ (BBY70) | *Mat a, ade2-101 his3-Δ200 leu2-Δ1 ura3-52 trp1-Δ63 lys2-801*; *oms1*::*klTRP1* [pRS416-OMS1$^{D326A}$] | This study |
| *oms1Δ* + Oms1$^{T327A}$ (BBY71) | *Mat a, ade2-101 his3-Δ200 leu2-Δ1 ura3-52 trp1-Δ63 lys2-801*; *oms1*::*klTRP1* [pRS416-OMS1$^{T327A}$] | This study |
| *oms1Δ* + Oms1$^{DT326/327AA}$ (BBY72) | *Mat a, ade2-101 his3-Δ200 leu2-Δ1 ura3-52 trp1-Δ63 lys2-801*; *oms1*::*klTRP1* [pRS416-OMS1$^{DT326/327AA}$] | This study |
| *oms1Δ* + Oms1$^{D326A}$ (2μ) (BBY74) | *Mat a, ade2-101 his3-Δ200 leu2-Δ1 ura3-52 trp1-Δ63 lys2-801*; *oms1*::*klTRP1* [pRS426-OMS1$^{D326A}$] | This study |
| *oms1Δ* + Oms1$^{D327A}$ (2μ) (BBY75) | *Mat a, ade2-101 his3-Δ200 leu2-Δ1 ura3-52 trp1-Δ63 lys2-801*; *oms1*::*klTRP1* [pRS426-OMS1$^{T327A}$] | This study |
| *oms1Δ* + Oms1$^{DT326/327AA}$ (2μ) (BBY76) | *Mat a, ade2-101 his3-Δ200 leu2-Δ1 ura3-52 trp1-Δ63 lys2-801*; *oms1*::*klTRP1* [pRS426-OMS1$^{DT326/327AA}$] | This study |

**TABLE 1:** Yeast strains used in this study.

was quenched with 1 M Tris/HCl (pH 7.4). After binding and washing, proteins were eluted with 0.1 M glycine (pH 2.8) and immediately neutralized with 1 M Tris (pH 11.5). For isolation of Mss51$^{SF}$, solubilized mitochondria were bound to preequilibrated Strep-Tactin Sepharose (IBA, Göttingen, Germany) for 1 h at 4°C. Bound protein complexes were eluted with elution buffer (5 mM desthiobiotin in digitonin wash buffer) for 15 min at 12°C for native analysis or with 0.1 M glycine (pH 2.8). For mass spectrometric (MS) analysis, samples were trichloroacetic acid (TCA) precipitated and resuspended in 20 mM Tris/HCl (pH 7.4), 100 mM NaCl, 10% (wt/vol) glycerol, and 5 mM EDTA.

### Mass spectrometry and SILAC

For SILAC, yeast strains auxotroph for lysine and arginine were used (*coa1Δarg4Δ*/ *coa1Δarg4Δ*Mss51$^{SF}$). Both strains were grown in medium containing heavy amino acids and medium containing natural (light) amino acids. Yeast cells were grown in SILAC medium (0.67% yeast nitrogen base, 20 mg/l histidine, 20 mg/l tryptophan, 20 mg/l adenine, 20 mg/l methionine, 20 mg/l uracil, 30 mg/l isoleucine, 30 mg/l tyrosine, 50 mg/l phenylalanine, 100 mg/ml leucine, 150 mg/l valine, 200 mg/l threonine, 200 mg/l proline, 20 mg/l [heavy or light, respectively] lysine, and 20 mg/l [heavy or light, respectively] arginine) supplied with 2% galactose

at 30°C. Proline (200 mg/l) was used to prevent the conversion of arginine into proline. Mitochondrial preparation followed the procedure described. Before complex isolation, mitochondria from cells grown on light and heavy media were mixed in a 1:1 ratio and solubilized together. For SILAC interactome analysis, eluted proteins were separated on 4–12% gradient SDS–PAGE gels (Invitrogen) and stained with colloidal Coomassie blue. Each gel lane was cut into 23 equal slices, and proteins therein were in-gel digested with trypsin (Promega; Shevchenko *et al.*, 2006). Tryptic peptides from each gel slice were analyzed by nanoflow HPLC coupled to nanoelectrospray LTQ-Orbitrap XL mass spectrometer (Thermo Fisher Scientific, Bremen, Germany) under standard conditions. Raw MS data were analyzed with MaxQuant and Andromeda (version 1.2.2.5; Cox and Mann, 2008; Cox *et al.*, 2011) using the *S. cerevisiae* UniProt reference protein database (version 29.11.11; 64,016 entries). Default double SILAC settings of MaxQuant were used with carbamidomethylation of cysteins and oxidation of methionines set as variable modifications. Results from MaxQuant were analyzed and visualized with R as described (Nikolov *et al.*, 2011).

### Extraction and HPLC analysis of hemes in cytochrome *c* oxidase

Complexes containing $Cox4^{ProtA}$ or $Mss51^{StrepFLAG}$ were purified from digitonin solubilized mitochondrial lysates using IgG-Sepharose or StrepTactin agarose, respectively. Hemes were extracted from purified complexes and analyzed as described previously (Hildenbeutel *et al.*, 2014). Briefly, samples were treated with 0.14% HCl in acetone, clarified by centrifugation, and analyzed by reverse-phase HPLC. To this end, extracts were loaded at 0.5 ml/min onto a 150-mm YMC ODS-A column (5 µm, 300 Å) at a Shimadzu Scientific HPLC Instrument in 75% buffer A (0.1% trifluoroacetic acid [TFA]/$H_2O$) and 25% buffer B (0.1% TFA/$CH_3CN$). Hemes were resolved using a 1%/min gradient from 55–75% buffer B and detected by ultraviolet/visible spectroscopy at 400 nm.

### BN–PAGE and in-gel activity staining

Mitochondria were solubilized in 1% digitonin, 20 mM Tris/HCl (pH 7.4), 5 mM EDTA, 100 mM NaCl, 10% (wt/vol) glycerol, and 2 mM PMSF to a final concentration of 1 mg/ml for 30 min at 4°C. Lysates were cleared by centrifugation (20,000 × *g*, 15 min, 4°C) before addition of 10× loading dye (5% Coomassie brilliant blue G-250, 500 mM 6-aminohexanoic acid, 100 mM Bis-Tris, pH 7.0) and separated on 4–13% polyacrylamide gradient gels with 4% stacking gel as described (Wittig *et al.*, 2007). Activity staining of respiratory chain complexes was performed at 30°C according to published procedures (Wittig *et al.*, 2007; Deckers *et al.*, 2014). For complex IV staining, gel stripes were incubated in 50 mM KPi (pH 7.4), 0.5 mg/ml diaminobenzidine, and 1 mg/ml reduced cytochrome *c*. Complex V staining was performed in 35 mM Tris/HCl, 220 mM glycine (pH 8.3), 8 mM ATP, 14 mM $MgSO_4$, and 0.2% $Pb(NO_3)_2$.

### In vivo labeling of mitochondrial translational products

In vivo labeling was performed in whole cells (grown on YPGal) in 40 mM KPi (pH 6.0), 2% galactose, 150 µg/ml cycloheximide, and 20 µCi of [$^{35}$S]methionine as described previously (Mick *et al.*, 2010). After 10 min (for pulse-only experiments) or 5 min (for pulse-chase experiments) of labeling at 30°C, reactions were stopped by addition of 10 mM unlabeled methionine. For chase experiments, samples were further incubated for the indicated times at 30°C, and proteins were extracted by alkaline treatment, precipitated with 10% TCA, and analyzed by SDS–PAGE and digital autoradiography.

### Isolated enzyme activity measurement

Spectrophotometric analysis of isolated respiratory chain complex activities was done using a Cary 50 Bio UV/Vis spectrophotometer as previously described (Deckers *et al.*, 2014). Cytochrome *c* reductase (CIII) activity was determined by the change of absorbance at 550 nm during reduction of cytochrome *c*. Mitochondria were added to sample buffer (40 mM potassium phosphate buffer, pH 7.4, 0.5 mM NADH) containing 0.02% (wt/vol) oxidized cytochrome *c*.

### Determination of mitochondrial respiration

Mitochondrial oxygen consumption rate was measured essentially as previously described with minor changes (Mourier *et al.*, 2014). Isolated yeast mitochondria (10 mg) were diluted in 2 ml of mitochondrial respiration buffer (120 mM sucrose, 220 mM mannitol, 2 mM 4-(2-hydroxyethyl)-1-piperazineethanesulfonic acid/HCl, 10 mM $KH_2PO_4$, 5 mM $MgCl_2$, 1 mM EGTA, pH 7.4) in an Oxygraph-2k (OROBOROS Instruments, Innsbruck, Austria). The oxygen consumption rate was measured using 1 mM NADH at 30°C. Oxygen consumption was assessed in the basal state and in the phosphorylating state with 1 mM ADP (state 3).

### Additional procedures

Standard techniques were applied for SDS–PAGE and Western blotting onto polyvinylidene fluoride membranes. All primary antibodies used were raised in rabbits. For detection and visualization of antibody–protein complexes on x-ray films, peroxidase-conjugated goat anti-rabbit IgG (Jackson ImmunoResearch) and enhanced chemiluminescence reagent (GE Healthcare) were used. Radioactive proteins were analyzed by digital autoradiography, and signals were quantified with the Image Quant software (GE Healthcare).

## ACKNOWLEDGMENTS

We are grateful to S. Callegari for a critical reading of the manuscript and R. Richter-Dennerlein, M. Deckers, and J. Dudek for discussions. We thank Monika Raabe and Uwe Plessmann for excellent technical assistance in mass spectrometry. M.H. received a postdoctoral stipend from the Wenner-Gren Foundation, Stockholm, Sweden. This work was supported by the Deutsche Forschungsgemeinschaft and the Max Planck Society (H.U. and P.R.).

## REFERENCES

Alkhaja AK, Jans DC, Nikolov M, Vukotic M, Lytovchenko O, Ludewig F, Schliebs W, Riedel D, Urlaub H, Jakobs S, *et al.* (2012). MINOS1 is a conserved component of mitofilin complexes and required for mitochondrial function and cristae organization. Mol Biol Cell 23, 247–257.

Bareth B, Dennerlein S, Mick DU, Nikolov M, Urlaub H, Rehling P (2013). The heme a synthase Cox15 associates with cytochrome c oxidase assembly intermediates during Cox1 maturation. Mol Cell Biol 33, 4128–4137.

Barrientos A, Korr D, Tzagoloff A (2002). Shy1p is necessary for full expression of mitochondrial COX1 in the yeast model of Leigh's syndrome. EMBO J 21, 43–52.

Barrientos A, Zambrano A, Tzagoloff A (2004). Mss51p and Cox14p jointly regulate mitochondrial Cox1p expression in Saccharomyces cerevisiae. EMBO J 23, 3472–3482.

Bauerschmitt H, Mick DU, Deckers M, Vollmer C, Funes S, Kehrein K, Ott M, Rehling P, Herrmann JM (2010). Ribosome-binding proteins Mdm38 and Mba1 display overlapping functions for regulation of mitochondrial translation. Mol Biol Cell 21, 1937–1944.

Bestwick M, Khalimonchuk O, Pierrel F, Winge DR (2010). The role of Coa2 in hemylation of yeast Cox1 revealed by its genetic interaction with Cox10. Mol Cell Biol 30, 172–185.

Bundschuh F, Hannappel A, Anderka O, Ludwig B (2009). Surf1, associated with Leigh syndrome in humans, is a heme-binding protein in bacterial oxidase biogenesis. J Biol Chem 284, 25735–25741.

Chen Y-C, Taylor EB, Dephoure N, Heo J-M, Tonhato A, Papandreou I, Nath N, Denko NC, Gygi SP, Rutter J (2012). Identification of a protein mediating respiratory supercomplex stability. Cell Metab 15, 348–360.
Cox J, Mann M (2008). MaxQuant enables high peptide identification rates, individualized p.p.b.-range mass accuracies and proteome-wide protein quantification. Nat Biotechnol 26, 1367–1372.
Cox J, Neuhauser N, Michalski A, Scheltema RA, Olsen JV, Mann M (2011). Andromeda: a peptide search engine integrated into the MaxQuant environment. J Proteome Res 10, 1794–1805.
Deckers M, Balleininger M, Vukotic M, Römpler K, Bareth B, Juris L, Dudek J (2014). Aim24 stabilizes respiratory chain supercomplexes and is required for efficient respiration. FEBS Lett 588, 2985–2992.
Decoster E, Simon M, Hatat D, Faye G (1990). The MSS51 gene product is required for the translation of the COX1 mRNA in yeast mitochondria. Mol Gen Genet 224, 111–118.
Fernández-Vizarra E, Tiranti V, Zeviani M (2009). Assembly of the oxidative phosphorylation system in humans: what we have learned by studying its defects. Biochim Biophys Acta 1793, 200–211.
Fontanesi F, Clemente P, Barrientos A (2011). Cox25 teams up with Mss51, Ssc1, and Cox14 to regulate mitochondrial cytochrome c oxidase subunit 1 expression and assembly in Saccharomyces cerevisiae. J Biol Chem 286, 555–566.
Fox TD (2012). Mitochondrial protein synthesis, import, and assembly. Genetics 192, 1203–1234.
Glerum D, Koerner T, Tzagoloff A (1995). Cloning and characterization of COX14, whose product is required for assembly of yeast cytochrome oxidase. J Biol Chem 270, 15585–15590.
Herrmann J, Funes S (2005). Biogenesis of cytochrome oxidase—sophisticated assembly lines in the mitochondrial inner membrane. Gene 354, 43–52.
Herrmann JM, Woellhaf MW, Bonnefoy N (2013). Control of protein synthesis in yeast mitochondria: the concept of translational activators. Biochim Biophys Acta 1833, 286–294.
Hildenbeutel M, Hegg EL, Stephan K, Gruschke S, Meunier B, Ott M (2014). Assembly factors monitor sequential hemylation of cytochrome b to regulate mitochondrial translation. J Cell Biol 205, 511–524.
Hutu DP, Guiard B, Chacinska A, Becker D, Pfanner N, Rehling P, van der Laan M (2008). Mitochondrial protein import motor: differential role of Tim44 in the recruitment of Pam17 and J-complex to the presequence translocase. Mol Biol Cell 19, 2642–2649.
Janke C, Magiera M, Rathfelder N, Taxis C, Reber S, Maekawa H, Moreno-Borchart A, Doenges G, Schwob E, Schiebel E, *et al.* (2004). A versatile toolbox for PCR-based tagging of yeast genes: new fluorescent proteins, more markers and promoter substitution cassettes. Yeast 21, 947–962.
Jia L, Dienhart M, Schramp M, McCauley M, Hell K, Stuart R (2003). Yeast Oxa1 interacts with mitochondrial ribosomes: the importance of the C-terminal region of Oxa1. EMBO J 22, 6438–6447.
Khalimonchuk O, Bestwick M, Meunier B, Watts TC, Winge DR (2010). Formation of the redox cofactor centers during Cox1 maturation in yeast cytochrome oxidase. Mol Cell Biol 30, 1004–1017.
Knop M, Siegers K, Pereira G, Zachariae W, Winsor B, Nasmyth K, Schiebel E (1999). Epitope tagging of yeast genes using a PCR-based strategy: more tags and improved practical routines. Yeast 15, 963–972.
Krüger V, Deckers M, Hildenbeutel M, van der Laan M, Hellmers M, Dreker C, Preuss M, Herrmann JM, Rehling P, Wagner R, *et al.* (2012). The mitochondrial oxidase assembly protein1 (Oxa1) insertase forms a membrane pore in lipid bilayers. J Biol Chem 287, 33314–33326.
Lemaire C, Guibet-Grandmougin F, Angles D, Dujardin G, Bonnefoy N (2004). A yeast mitochondrial membrane methyltransferase-like protein can compensate for oxa1 mutations. J Biol Chem 279, 47464–47472.
Manthey GM, McEwen JE (1995). The product of the nuclear gene PET309 is required for translation of mature mRNA and stability or production of intron-containing RNAs derived from the mitochondrial COX1 locus of Saccharomyces cerevisiae. EMBO J 14, 4031–4043.
Mayorga JP, Camacho-Villasana Y, Shingu-Vazquez M, Garcia-Villegas R, Zamudio-Ochoa A, Garcia-Guerrero AE, Hernandez G, Perez-Martinez X (2016). A novel function of Pet54 on regulation of Cox1 synthesis in *Saccharomyces cerevisiae* mitochondria. J Biol Chem 2016, jbc. M116.721985.
Meisinger C, Pfanner N, Truscott KN (2006). Isolation of yeast mitochondria. Methods Mol Biol 313, 33–39.
Mick DU, Fox TD, Rehling P (2011). Inventory control: cytochrome c oxidase assembly regulates mitochondrial translation. Nat Rev Mol Cell Biol 12, 14–20.
Mick DU, Vukotic M, Piechura H, Meyer HE, Warscheid B, Deckers M, Rehling P (2010). Coa3 and Cox14 are essential for negative feedback regulation of COX1 translation in mitochondria. J Cell Biol 191, 141–154.
Mick DU, Wagner K, van der Laan M, Frazier AE, Perschil I, Pawlas M, Meyer HE, Warscheid B, Rehling P (2007). Shy1 couples Cox1 translational regulation to cytochrome c oxidase assembly. EMBO J 26, 4347–4358.
Mourier A, Ruzzenente B, Brandt T, Kühlbrandt W, Larsson N-G (2014). Loss of LRPPRC causes ATP synthase deficiency. Hum Mol Genet 23, 2580–2592.
Nikolov M, Stützer A, Mosch K, Krasauskas A, Soeroes S, Stark H, Urlaub H, Fischle W (2011). Chromatin affinity purification and quantitative mass spectrometry defining the interactome of histone modification patterns. Mol Cell Proteomics 10, M110.005371.
Ong S-E, Blagoev B, Kratchmarova I, Kristensen DB, Steen H, Pandey A, Mann M (2002). Stable isotope labeling by amino acids in cell culture, SILAC, as a simple and accurate approach to expression proteomics. Mol Cell Proteomics 1, 376–386.
Ott M, Prestele M, Bauerschmitt H, Funes S, Bonnefoy N, Herrmann JM (2006). Mba1, a membrane-associated ribosome receptor in mitochondria. EMBO J 25, 1603–1610.
Pérez-Martínez X, Broadley SA, Fox TD (2003). Mss51p promotes mitochondrial Cox1p synthesis and interacts with newly synthesized Cox1p. EMBO J 22, 5951–5961.
Pérez-Martínez X, Butler CA, Shingú-Vázquez M, Fox TD (2009). Dual functions of Mss51 couple synthesis of Cox1 to assembly of cytochrome c oxidase in Saccharomyces cerevisiae mitochondria. Mol Biol Cell 20, 4371–4380.
Pfeffer S, Woellhaf MW, Herrmann JM, Förster F (2015). Organization of the mitochondrial translation machinery studied in situ by cryoelectron tomography. Nat Commun 6, 6019.
Pierrel F, Bestwick ML, Cobine PA, Khalimonchuk O, Cricco JA, Winge DR (2007). Coa1 links the Mss51 post-translational function to Cox1 cofactor insertion in cytochrome c oxidase assembly. EMBO J 26, 4335–4346.
Pierrel F, Khalimonchuk O, Cobine PA, Bestwick M, Winge DR (2008). Coa2 is an assembly factor for yeast cytochrome c oxidase biogenesis that facilitates the maturation of Cox1. Mol Cell Biol 28, 4927–4939.
Rehling P, Model K, Brandner K, Kovermann P, Sickmann A, Meyer HE, Kühlbrandt W, Wagner R, Truscott KN, Pfanner N (2003). Protein insertion into the mitochondrial inner membrane by a twin-pore translocase. Science 299, 1747–1751.
Richter-Dennerlein R, Dennerlein S, Rehling P (2015). Integrating mitochondrial translation into the cellular context. Nat Rev Mol Cell Biol 16, 586–592.
Roloff GA, Henry MF (2015). Mam33 promotes cytochrome c oxidase subunit I translation in *Saccharomyces cerevisiae* mitochondria. Mol Biol Cell 26, 2885–2894.
Shevchenko A, Tomas H, Havlis J, Olsen JV, Mann M (2006). In-gel digestion for mass spectrometric characterization of proteins and proteomes. Nat Protoc 1, 2856–2860.
Sikorski R, Hieter P (1989). A system of shuttle vectors and yeast host strains designed for efficient manipulation of DNA in Saccharomyces cerevisiae. Genetics 122, 19–27.
Soto IC, Fontanesi F, Liu J, Barrientos A (2012). Biogenesis and assembly of eukaryotic cytochrome c oxidase catalytic core. Biochim Biophys Acta 1817, 883–897.
Strogolova V, Furness A, Robb-McGrath M, Garlich J, Stuart RA (2012). Rcf1 and Rcf2, members of the hypoxia-induced gene 1 protein family, are critical components of the mitochondrial cytochrome bc1-cytochrome c oxidase supercomplex. Mol Cell Biol 32, 1363–1373.
Szyrach G, Ott M, Bonnefoy N, Neupert W, Herrmann JM (2003). Ribosome binding to the Oxa1 complex facilitates co-translational protein insertion in mitochondria. EMBO J 22, 6448–6457.
Taanman J, Williams S (2001). Assembly of cytochrome c oxidase: what can we learn from patients with cytochrome c oxidase deficiency? Biochem Soc Trans 29, 446–451.
Vukotic M, Oeljeklaus S, Wiese S, Vögtle F-N, Meisinger C, Meyer HE, Zieseniss A, Katschinski DM, Jans DC, Jakobs S, *et al.* (2012). Rcf1 mediates cytochrome oxidase assembly and respirasome formation, revealing heterogeneity of the enzyme complex. Cell Metab 15, 336–347.
Wittig I, Karas M, Schägger H (2007). High resolution clear native electrophoresis for in-gel functional assays and fluorescence studies of membrane protein complexes. Mol Cell Proteomics 6, 1215–1225.